Supplement of Compositions and mixing states of aerosol particles by aircraft observations in the Arctic springtime, 2018

Kouji Adachi[1], Naga Oshima[1], Sho Ohata[2,3,4], Atsushi Yoshida[2], Nobuhiro Moteki[2], and Makoto Koike[2]

[1] Department of Atmosphere, Ocean, and Earth System Modeling Research, Meteorological Research Institute, Tsukuba, Japan
[2] Department of Earth and Planetary Science, Graduate School of Science, The University of Tokyo, Tokyo, Japan
[3] Institute for Space–Earth Environmental Research, Nagoya University, Nagoya, Japan
[4] Institute for Advanced Research, Nagoya University, Nagoya, Japan

Correspondence to: Kouji Adachi (adachik@mri-jma.go.jp)

Figures S1 to S11.

Table S1.

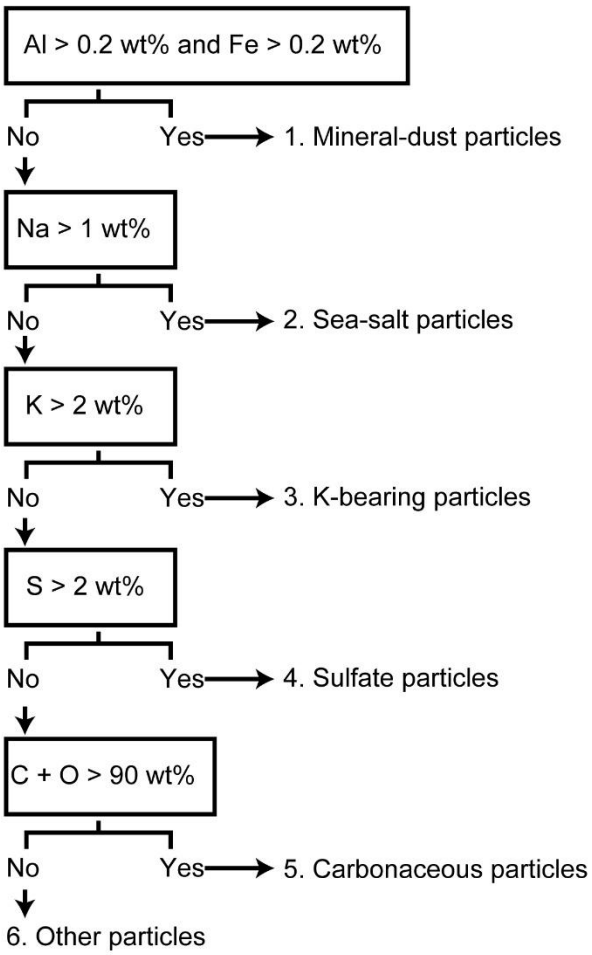

Figure S1. Flow chart to classify the individual particles into six categories based on the STEM-EDS measurements. This flow chart is nearly the same as that in Adachi et al. (2020), but we excluded primary biological aerosol particles (P-bearing particles) in the current study.

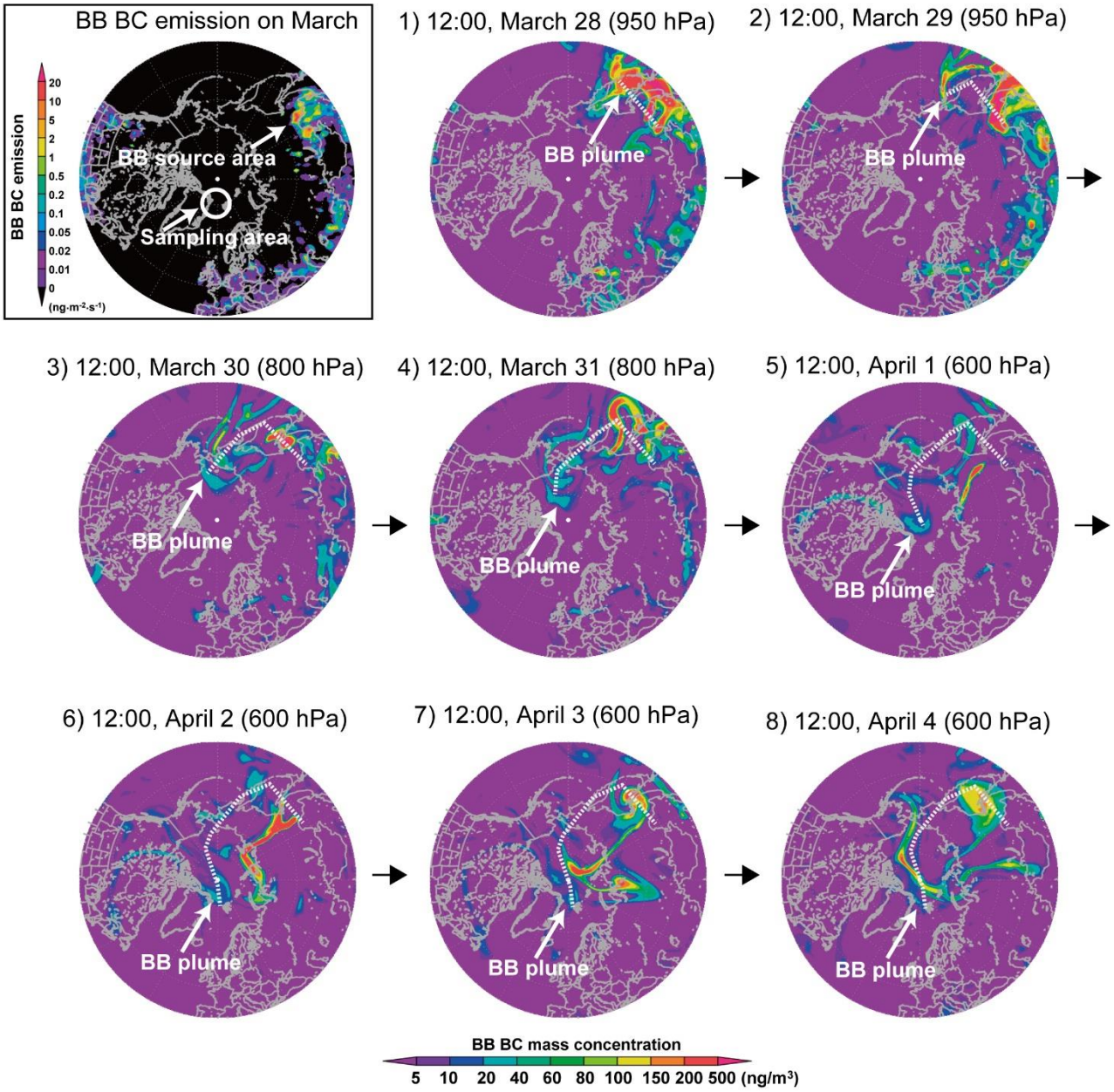

Figure S2. Black carbon (BC) emissions from biomass burning (BB) in March 2018 (upper left) and horizontal distributions of the mass concentration of BC originating from BB from 28 March to 4 April 2018 at 12:00 UTC (1-8). The dotted lines indicate the transport pathway of the BB BC plume that reached the sampling area between 2 and 4 April. Note that the pressure (altitude) levels are different in each panel depending on the air mass transport.

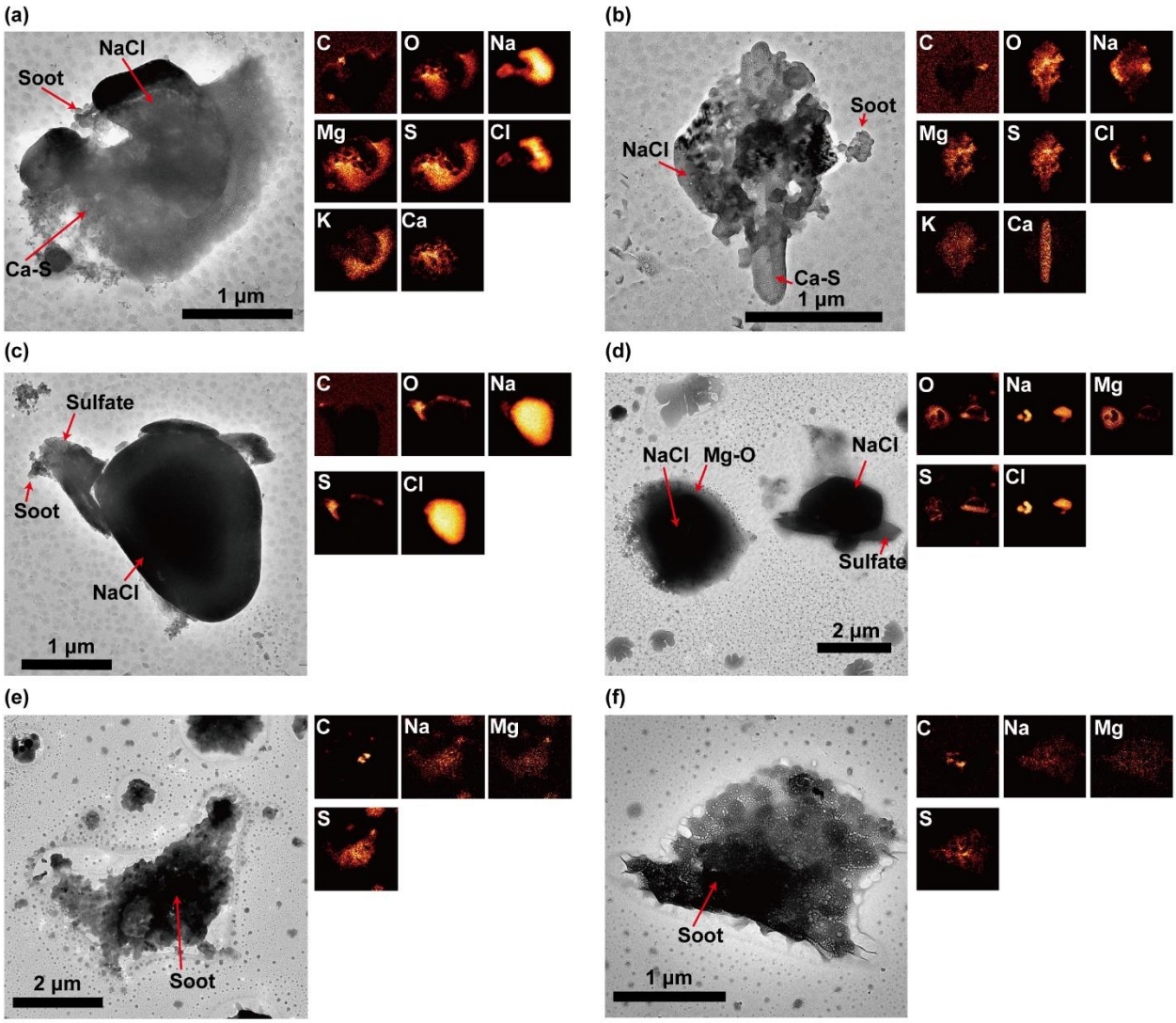

Figure S3. TEM and elemental mapping images of the sea-salt particles. The particles in (a), (b), (c), and (d) were collected from 10:00-10:19, 30 March, 2018, and those in (e) and (f) were collected from 14:40-14:59, 31 March. The left TEM image in each panel shows the sea-salt particles mixed with various grains. Elemental mapping images of the TEM areas for the detected elements are shown on the right in each panel. Chlorine was not detected in the particles in (e) and (f) because of Cl replacement with sulfate in the atmosphere.

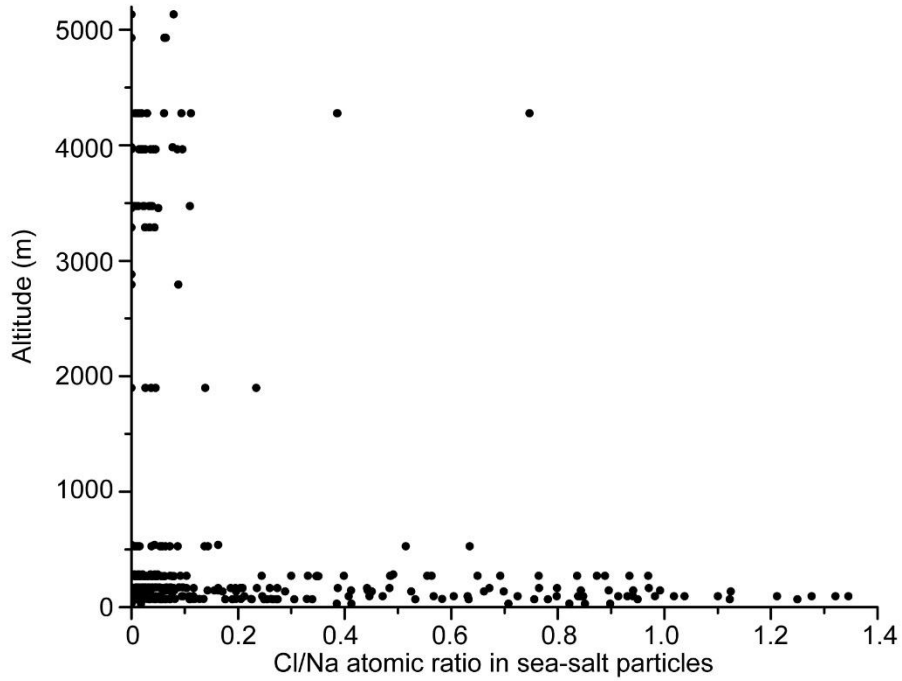

Figure S4. Ratios of Cl to Na in the atomic ratio for all individual sea-salt particles. Chlorine was largely lost in the particles collected above 1000 m.

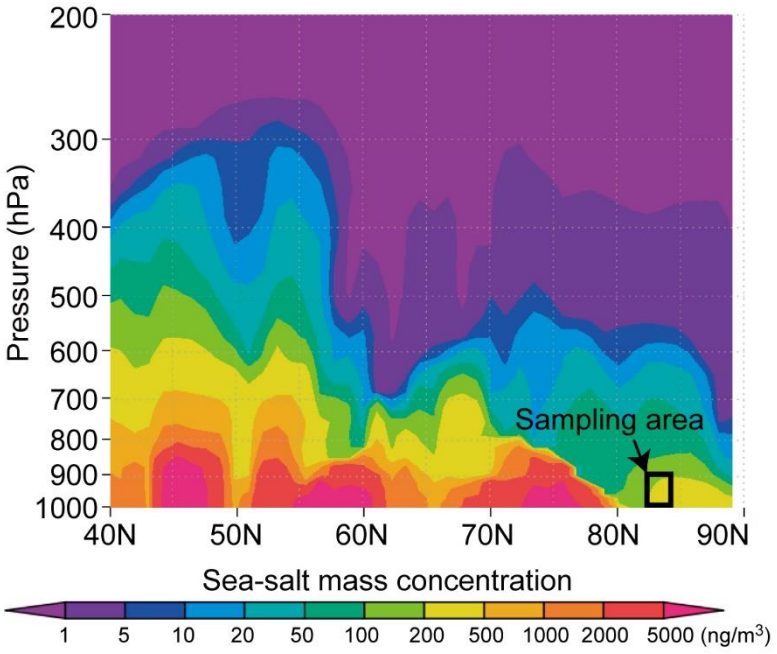

Figure S5. Example model result of the vertical distribution of the sea-salt mass concentration on 12:00 UTC, 30 March 2018 at 0° E longitude. The sea-salt number fractions in the TEM analysis were relatively high on that day. The sampling area is shown in a black square.

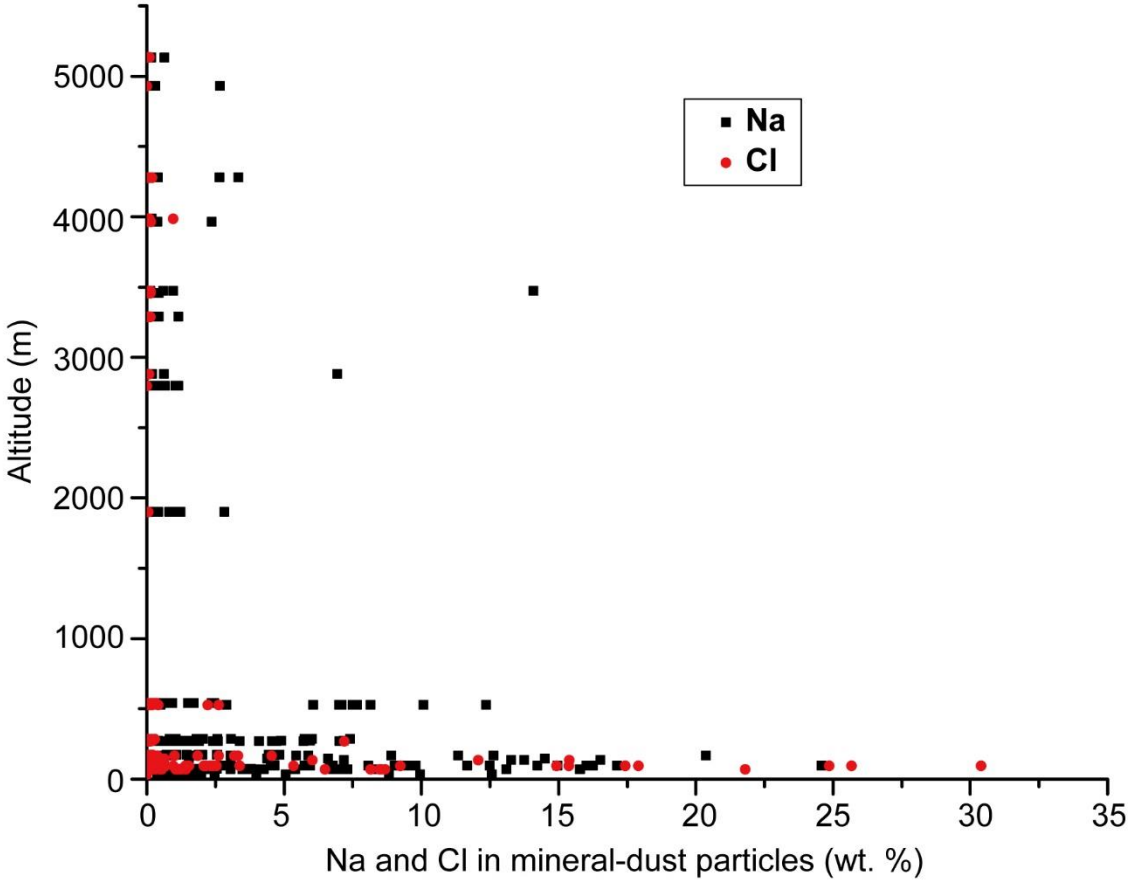

Figure S6. Weight percent of Na (black) and Cl (red) within all mineral-dust particles along with their sampling altitude. The sea-salt fractions within the individual mineral-dust particles are high at a low altitude.

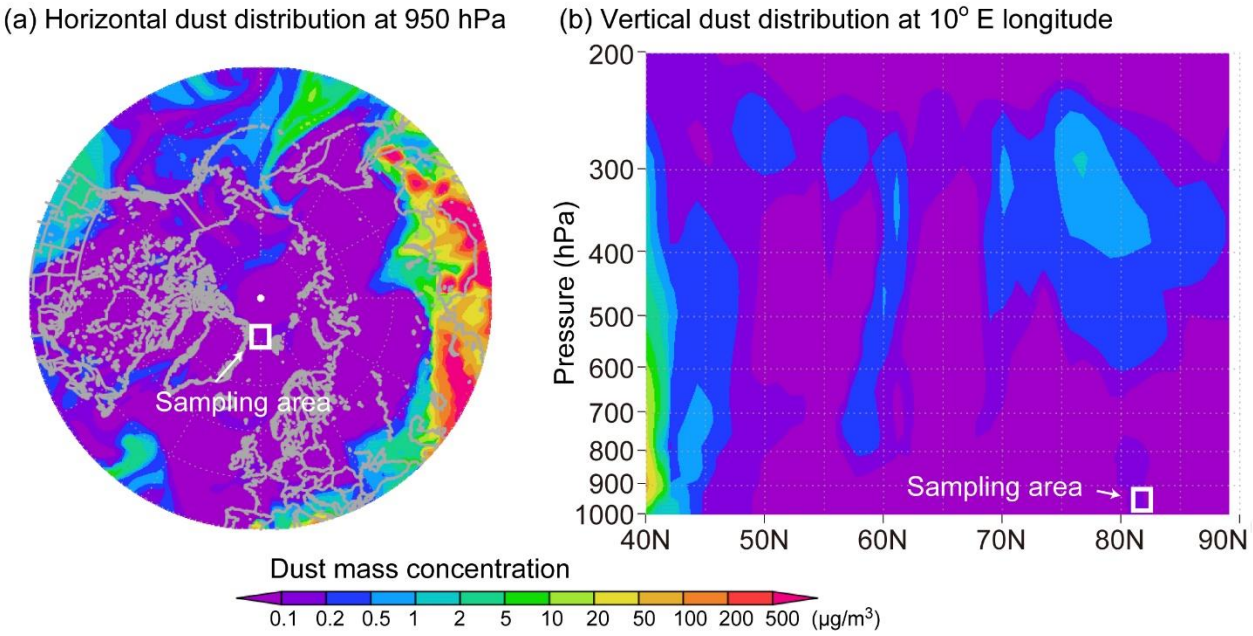

Figure S7. Example model results of the (a) horizontal and (b) vertical distributions of the mineral-dust mass concentration on 12:00 UTC, 30 March 2018. The mineral-dust number fractions in the TEM analysis were relatively high on that day, but no dust plume was detected in the model. The vertical distribution is shown along the 10° E longitude. The sampling area is shown in the white squares.

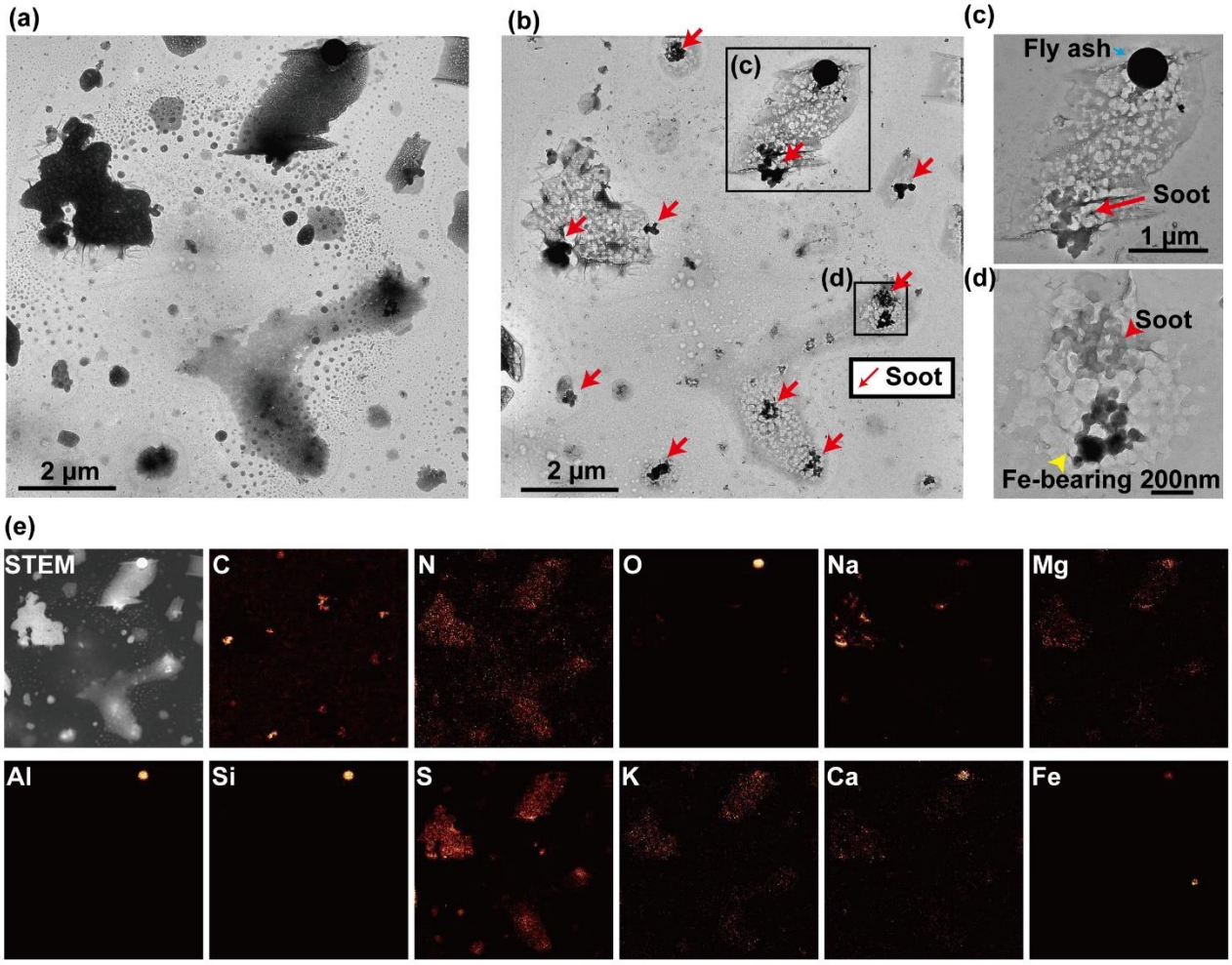

Figure S8. TEM and elemental mapping images of the sulfate particles containing inclusions. (a) TEM image before the mapping analysis and (b) after the mapping analysis. Electron-beam exposure removed sulfate, and the inclusions became more apparent. (c) A particle in the image (b) with fly-ash and soot inclusions. (d) A particle with Fe-aggregate and soot inclusions. (e) Elemental mapping images of the TEM areas of the detected elements. The C distributions in the mapping image correspond to the soot particles. The fly-ash particle in (c) includes O, Al, and Si as its main components. Fe is apparent in the Fe-aggregate particle in (d). The sample was collected from 14:40-14:59, 31 March 2018.

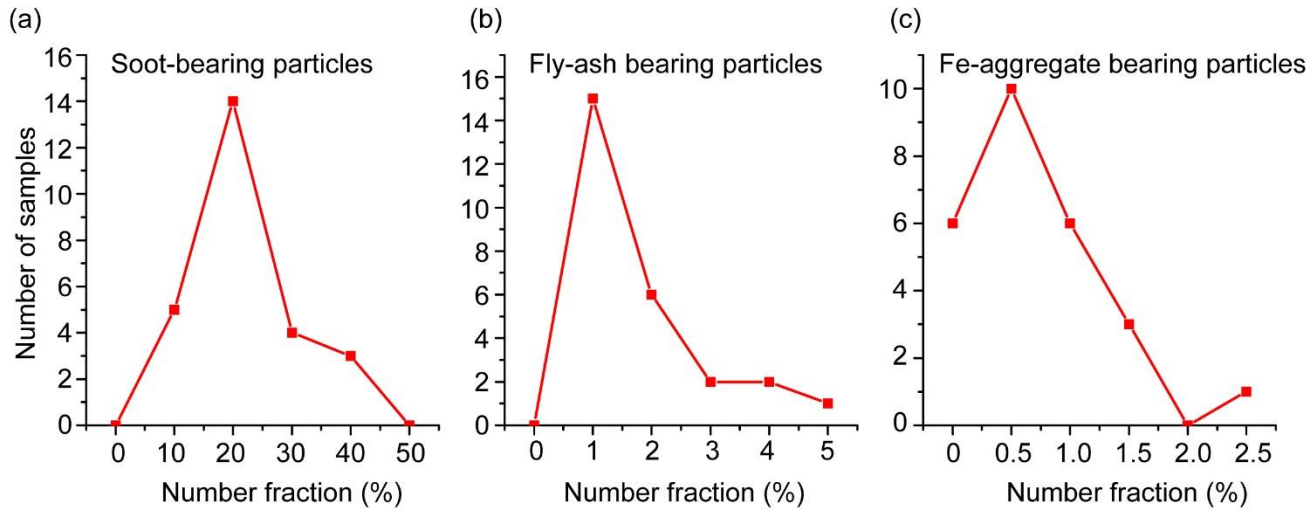

Figure S9. Histogram of the number fractions of the particles containing inclusions. (a) Soot-bearing particle number fractions. (b) Fly-ash bearing particle number fractions. (c) Fe-aggregate-bearing particle number fractions. The average values of these number fractions are 17%, 1.4%, and 0.5%, respectively.

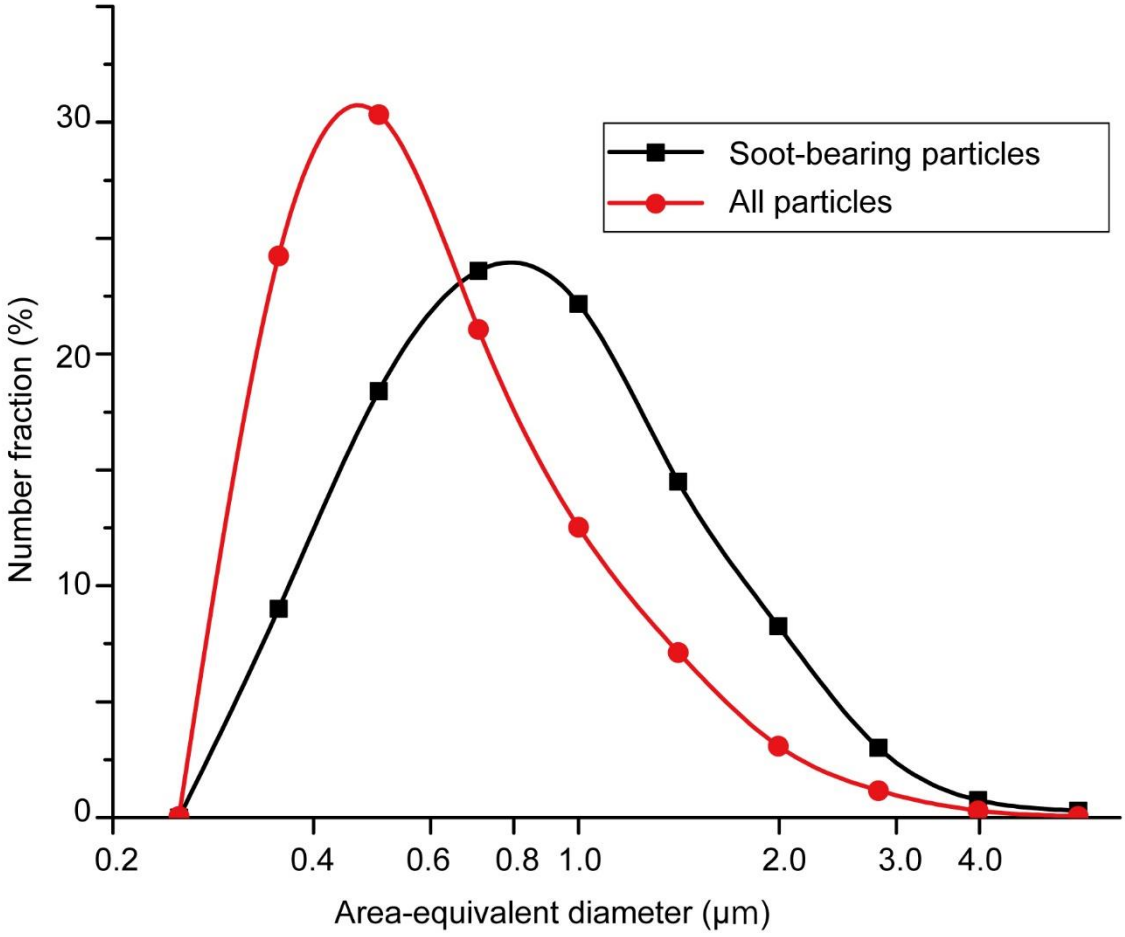

Figure S10. Size distributions of the soot-bearing particles (black line) and all particles (red line). The size bins are shown on a log scale (< 0.25, 0.25-0.35, 0.35-0.5, 0.5-0.71, 0.71-1.00, 1.00-1.41, 1.41-2.00, 2.00-2.82, 2.82-3.98, and >3.98 μm). The sizes of the soot-bearing particles reflect those of their host particles. The numbers of all particles and soot-bearing particles are 7844 and 1331, respectively.

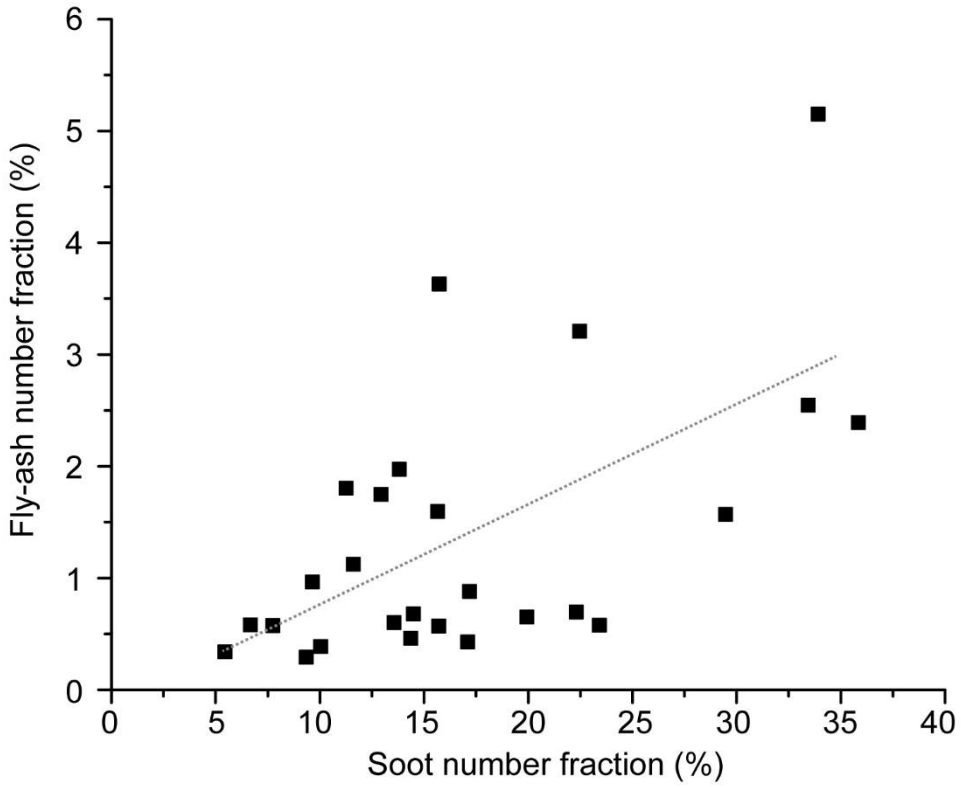

Figure S11. The relation between the number fractions of the soot and fly-ash particles within each TEM sample. R^2=0.35.

SI Table 1. Sampling date and time, number fractions of the main components and inclusions, and sampling point information.

Sampling		Main components (Number fractions %)						Inclusions (%)			Sampling points			
Sampling date	Start time (UTC)	Mineral dust	Sea salt	K-bearing	Sulfate	Carbonaceous	Other	Soot	Fly ash	Fe-bearing	Altitude (m)	Latitude	Longitude	Biomass burning plume
25-Mar	14:00	8	23	3	65	0	1	22	0.7	0.3	34	81.59619	-16.6591	
25-Mar	15:40	9	9	4	75	0	3	14	2.0	1.3	541	81.50161	-9.51961	
25-Mar	16:40	5	3	5	86	1	1	23	0.6	0.9	2797	81.50279	-8.5448	
26-Mar	12:40	5	21	1	66	5	1	16	0.6	0.3	275	82.56004	-14.1693	
26-Mar	13:00	2	14	0	71	9	3	10	0.4	0.4	147	82.50293	-12.742	
26-Mar	15:00	1	6	6	70	12	5	14	0.5	1.4	5133	82.49932	-14.4512	
27-Mar	14:20	4	14	3	62	12	5	17	0.9	0.4	271	82.46931	-18.3625	
27-Mar	14:40	6	12	4	50	29	0	11	1.8	0.0	137	82.50295	-16.564	
27-Mar	15:40	3	9	6	41	28	13	17	0.4	0.0	1901	82.50208	-16.6887	
30-Mar	10:00	11	39	3	45	1	1	10	1.0	0.0	96	82.50611	6.9813	
30-Mar	10:20	7	31	2	45	15	0	9	0.3	0.3	71	82.50614	11.19458	
30-Mar	10:40	8	33	3	51	5	1	13	1.7	0.0	169	82.50461	16.70325	
30-Mar	11:20	2	3	3	80	8	5	16	1.6	1.0	3986	82.73554	16.05952	
31-Mar	14:20	5	39	2	45	10	0	36	2.4	1.0	74	84.04489	-12.0732	
31-Mar	14:40	5	58	0	29	7	0	34	5.2	2.1	174	83.57378	-14.6603	
31-Mar	15:00	5	33	3	43	16	0	33	2.5	0.3	73	83.08185	-16.9647	
2-Apr	10:20	2	1	4	69	4	19	5	0.3	0.0	2883	81.37321	-11.7275	
2-Apr	10:40	1	2	37	53	4	2	14	0.7	0.7	4930	81.07854	-6.82414	BB
2-Apr	11:00	1	1	1	45	30	21	8	0.6	0.3	3459	80.64019	-1.39979	
3-Apr	8:00	1	6	4	77	8	4	7	0.6	0.0	3475	81.37747	-11.6657	
3-Apr	8:30	2	6	12	60	12	8	12	1.1	0.7	4279	80.98157	-4.74884	BB
3-Apr	9:00	5	15	2	37	29	11	16	3.6	0.4	531	80.83391	-5.49512	
3-Apr	11:00	4	15	2	58	5	16	22	3.2	0.7	286	80.91201	-7.04061	
4-Apr	8:00	3	3	3	64	26	2	20	0.7	0.7	3291	81.37874	-11.6985	
4-Apr	8:30	2	4	11	76	2	5	14	0.6	0.3	3966	81.07125	-3.44506	BB
4-Apr	9:00	6	13	1	71	6	3	29	1.6	0.3	271	81.0339	-2.40188	
Average		4	16	5	59	11	5	17	1.4	0.5				